Flying gyroless around Mars: a SW update for Mars Express

Juan Manuel García [1, 2], Carlos Bielsa[1, 3], Michael Mueller [1]

[1] *European Space Operations Centre, ESA, Darmstadt, Germany*
[2] *Flight Dynamics and Operations, GMV-INSYEN AG, Darmstadt, Germany*
[3] *IMS Space Consultancy GmbH, Darmstadt, Germany*

In early 2017, four out of the six gyros on board Mars Express showed signs of aging such that, if the gyro usage was not reduced, a worst-case end of mission could happen as soon as late 2018. In April 2018, the Mission Control Team working at ESOC upgraded the Mars Express AOCS On-Board Software incorporating the Gyroless Attitude Estimator from the Rosetta mission. Today, Mars Express is flying gyroless nominally around Mars, saving its gyros for moments where they are strictly necessary. The duty cycle of the IMUs has been reduced significantly, making them no longer the driver for the mission end date. This paper presents the Flight Dynamics work related to the software upgrade, from the initial feasibility studies to the successful implementation and validation of the solution.

Keywords: Mars Express, gyroless attitude estimator, gyrostellar attitude estimator, AOCS On-Board Software, Rosetta, gyros

1. Introduction

Mars Express (MEX) was the first ESA mission to another planet in the Solar System. Launched in 2003, it began its science operations around Mars in 2004 and is still operating today after several mission extensions.

In early 2017, four out of the six gyros on board MEX started showing signs of aging. The on-board attitude estimation requires at least three working gyros. A preliminary analysis showed that, were the gyro usage not reduced, end of mission due to gyro unavailability could happen as early as late 2018.

Substantial elements of MEX design, and in particular, of its Attitude and Orbit Control Subsystem (AOCS) on-board software (OBSW), were inherited from Rosetta (ROS), another ESA mission that flew to comet 67P/C-G. Owing to its higher complexity, ROS AOCS OBSW included some extra elements compared to MEX; amongst them, a gyroless attitude estimator intended to spare gyro lifetime during its long interplanetary cruise phase. Given the commonalities between ROS and MEX AOCS software, the possibility to adapt the ROS gyroless estimator design for MEX was put forward as a quick and affordable solution to the MEX gyro lifetime problem. In addition, if this solution proved feasible, it could be directly implemented by the operations control centre, which, having been in charge of the ROS operations, was already familiar with its AOCS OBSW.

This idea was studied and implemented by the European Space Operations Centre (ESOC), with support from the spacecraft manufacturer AIRBUS, between August 2017 and April 2018 and was operationally deployed in mid-April 2018. Since then, MEX is performing science operations using the gyroless estimator with similar pointing performances. The gyro duty cycle has been reduced to below 10% and the mission lifetime is no longer expected to be driven by the remaining lifetime of the gyros.

This paper presents the Flight Dynamics work related to the update of the AOCS OBSW. Section 2 provides a high-level overview of the attitude estimation process. Section 3 covers the initial feasibility study, whose main aim was to analyse whether the ROS gyroless estimator was applicable in MEX with similar pointing error performances. Section 4 covers the AOCS OBSW modification design. Section 5 is dedicated to the tuning of the gyroless attitude estimator. Finally, section 6 describes the operational phase in of the new AOCS OBSW and shows some in-flight results collected during the first week of gyroless operations.

2. Formulation of the attitude estimators

2.1. Gyrostellar Estimator (GSE)

The gyrostellar estimator, the only original estimator on board MEX, estimates the attitude of the spacecraft based on gyros and Star Tracker (STR) measurements. It is based on a simplified Multiplicative Extended Kalman Filter (MEKF) with constant covariance.

The estimator state vector contains the four S/C attitude quaternion components and three components for the gyro drift along the S/C axes, i.e. $\bar{X} = \{q_1, q_2, q_3, q_4, d_x, d_y, d_z\}$. Internally, however, the prediction and correction steps are based on the small angle approximation and rely on the representation of the attitude error as three angular depointings around each S/C axis. The state vector correction contains these three depointing errors plus the three drift correction components $\bar{X}^{cor} = \{\theta_x^{cor}, \theta_y^{cor}, \theta_z^{cor}, d_x^{cor}, d_y^{cor}, d_z^{cor}\}$

The filter prediction step runs at 8Hz. It propagates the attitude using the rates measured by the gyros corrected with the estimated gyro drift:

$$\theta_i^{pred} = \left(\omega_i - \hat{d}_{i_{n-1}}\right)\Delta T_{8Hz} \; for \; i = x, y, z \tag{1}$$

$$\hat{d}_{n|n-1} = \hat{d}_{n-1} \tag{2}$$

where ω_i are the rates as read from the gyros and the notation $\hat{a}_{n|n-1}$ indicates the prediction of quantity a for time step n based on the knowledge from time step n-1.

The filter update step runs at 2Hz, which is the frequency at which STR measurements are acquired. The attitude state is updated based on the difference between the measured star coordinates and the predicted star coordinates in the STR CCD, applying the following gain matrix (where H_n is the observation matrix):

$$K_n = P_0 \cdot H_n^T \cdot (H_n \cdot P_0 \cdot H_n^T + W)^{-1} \tag{3}$$

Notice that the state error covariance matrix P_0 is kept constant and is the main subject of the estimator tuning. The stellar measurement covariance matrix W is also assumed to be constant and is obtained from the sensor performance model.

2.2. Gyroless Estimator (GLE)

The gyroless estimator estimates the attitude based solely on STR measurements. It follows the same principle as the gyrostellar estimator. However, owing to the lack of gyro measurements, the propagation of the attitude between STR measurements is performed through a dynamic model (discrete integration of the Euler equations of motion):

$$\begin{aligned}
\hat{\omega}_{x_{n|n-1}} &= \hat{\omega}_{x_{n-1}} + \frac{\Delta t}{I_{xx}}\left(T_{n-1_x} - (I_{zz} - I_{yy})\hat{\omega}_{y_{n-1}}\hat{\omega}_{z_{n-1}} - \hat{\omega}_{y_{n-1}}\hat{h}_{RW_{z_{n-1}}} + \hat{\omega}_{z_{n-1}}\hat{h}_{RW_{y_{n-1}}}\right) \\
\hat{\omega}_{y_{n|n-1}} &= \hat{\omega}_{y_{n-1}} + \frac{\Delta t}{I_{yy}}\left(T_{n-1_y} - (I_{xx} - I_{zz})\hat{\omega}_{x_{n-1}}\hat{\omega}_{z_{n-1}} - \hat{\omega}_{z_{n-1}}\hat{h}_{RW_{x_{n-1}}} + \hat{\omega}_{x_{n-1}}\hat{h}_{RW_{z_{n-1}}}\right) \quad (4) \\
\hat{\omega}_{z_{n|n-1}} &= \hat{\omega}_{z_{n-1}} + \frac{\Delta t}{I_{zz}}\left(T_{n-1_z} - (I_{yy} - I_{xx})\hat{\omega}_{x_{n-1}}\hat{\omega}_{y_{n-1}} - \hat{\omega}_{x_{n-1}}\hat{h}_{RW_{y_{n-1}}} + \hat{\omega}_{y_{n-1}}\hat{h}_{RW_{x_{n-1}}}\right)
\end{aligned}$$

where T_{n-1} is the torque applied to the S/C by the actuators at time t_{n-1} and $\hat{h}_{RW_{n-1}}$ is the estimated angular momentum of the reaction wheels at time t_{n-1}. Notice that external torques are not accounted for and that only the diagonal terms of the S/C inertia tensor are considered. The rest of the process is identical to the GSE estimation.

The insertion of the dynamic model creates a qualitative difference in the way the S/C control loop is configured: because the RW estimated angular momenta are used to predict the rates, a coupling between the attitude and the RW angular momentum estimators is created.

3. Feasibility study

Despite the similarities between the ROS and MEX platforms, the intended use of the GLE for both missions presented two important differences in terms of flight profile and external torques, summarized in Table 1. This is because ROS used the GLE only during its deep space cruise phase, while MEX requires its use for science operations around Mars with higher attitude rates and significant external torque due to Mars gravity gradient at pericentre. These differences alone could have been enough to invalidate the use of the ROS gyroless estimator in MEX. For this reason, an initial feasibility study was performed in order to assess whether the estimator could still be applied in this different regime.

Table 1: Differences between ROS and MEX gyroless use cases

	MEX	**ROS**
Attitude rate	$\sim 0.3\ °/s$	$\sim 6 \cdot 10^{-4}\ °/s$
External torques	$\sim 0.08\ Nm$	$\sim 10^{-4} Nm$

3.1. The analysis tool

The Command Emulator is the tool that was used by Flight Dynamics for the dynamic studies related to the MEX gyroless software upgrade. It consists of an articulated rigid body attitude dynamics simulator combined with an AOCS OBSW emulator that replicates the real AOCS software of the mission. Its main purpose is AOCS command validation, which is why some of its models are not fully representative of the real S/C behavior. In particular, flexible dynamics are not modelled and the hardware models of the different units are normally simplified. For this reason, before proceeding with the study of the GLE estimator, the validity of the emulator as an analysis tool was checked using real MEX telemetry data. Various flight profiles were compared to gain confidence on the tool and understand its limitations.

3.2. Preliminary performance analysis

The purpose of the preliminary performance analysis was to obtain an initial idea of the performances that could be expected from an implementation of the ROS gyroless estimator on MEX. Based on the differences reported in Table 1, the aim was to analyse the behaviour of the ROS gyroless estimator concept under typical MEX flight regime conditions, i.e., high rates

and significant external torques due to Mars gravity gradient. With this idea in mind, the following pointing profiles were analysed:

1. Earth pointing attitude around pericentre (low rates, relevant external torques)
2. Inertial pointing around a pericentre (null rates, high external torques)
3. Z-axis Nadir pointing around a pericentre (high rates, low external torques)
4. Offset axis Nadir pointing around a pericentre (high rates, maximum external torques)

For each of these attitude profiles, four Emulator runs were executed and their performances were compared:

A. GSE as in current flight configuration (used as reference case)
B. GLE as in ROS (as described in 2.2)
C. GLE with an enhanced prediction model including the Gravity Gradient torque
D. GLE with a simplified constant rate prediction model

Runs B, C, and D were then compared against the reference along the following metrics:

- Attitude Measurement Error (AME): estimated vs simulated attitude
- Rate Measurement Error (RME): estimated vs simulated rate
- Attitude Control Error (ACE): estimated vs commanded attitude
- Rate Control Error (RCE): estimated vs commanded rate
- Attitude Pointing Error (APE): commanded vs simulated attitude

Since the idea was to stay as close as possible to the Rosetta design, the analysis was mainly focused on run B. The purpose of run C was to analyse the potential gain from including the main external torque into the on-board prediction model. In contrast, the purpose of run D was to assess the performance degradation from using a much simpler prediction model (constant rate, which would have decoupled the attitude and RW angular momentum estimators, as in the GSE). For this initial analysis, the estimator tuning was kept as in ROS. Since the ROS tuning process was only driven by response time considerations and was independent of the physical or flight-profile dependent properties of the S/C, there was no reason to believe that the tuning would be invalid for MEX (although it could be suboptimal).

This initial study yielded the following main conclusions:

- The ROS GLE estimator, with identical implementation and tuning, performs very similarly to the MEX GSE estimator except around Solar Array (SA) repositionings, where the estimator error is larger due to the high angular acceleration
- Replacing the dynamic prediction model with a constant rate prediction model results in significant performance degradation
- The benefit of introducing an on-board Gravity Gradient model is not enough to justify the additional OBSW complexity

Fig. 1 is one example of the results leading to the first conclusion. It shows the comparison of the AME with GSE and GLE estimators for a Z-axis Nadir pointing flight profile. It can be seen that the achieved performance is very similar in magnitude except for the solar array repositioning spikes, were the gyroless error is bigger. This is caused by the GLE rate estimation capturing the effect of the solar array motion acceleration too slowly, thus inducing a higher AME.

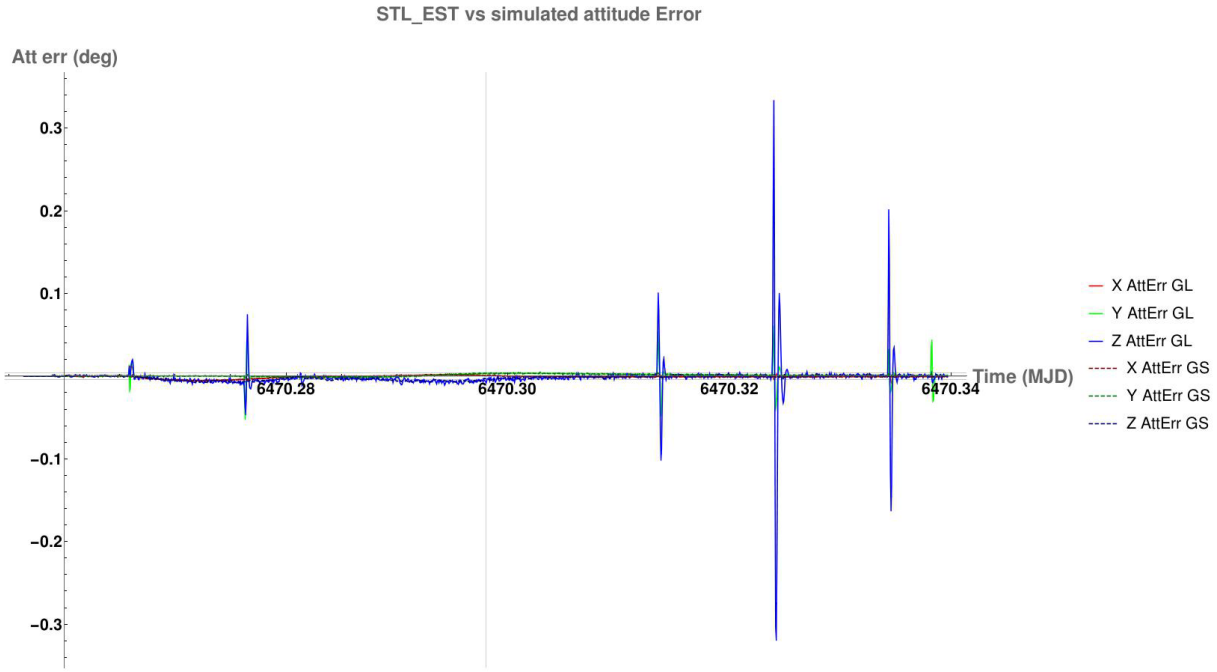

Figure 1: AME during solar array repositionings around nadir pointing profile

Fig. 2 shows an example of the ACE behavior when a constant rate prediction model is used. The performance degrades especially during solar array repositionings, where the time required to damp the effect of the sudden acceleration is much higher.

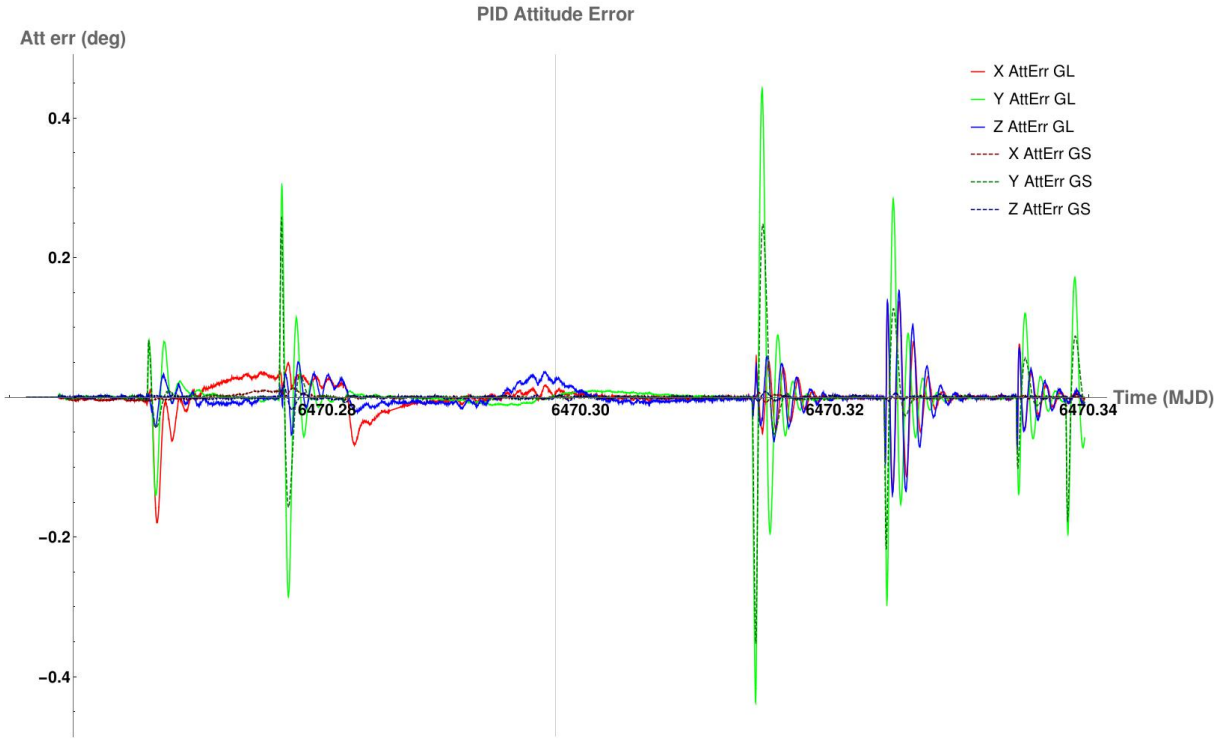

Figure 2: ACE during nadir pointing profile, GS vs GL with constant rate prediction

Fig. 3 shows an example of the AME when a gravity gradient prediction model is introduced in the GLE prediction step, for a flight profile with high gravity gradient torques. The performance is closer to the one given by the GSE both in stability (smaller oscillations) and in

magnitude. However, the obtained gain is not significant enough to justify the additional complexity.

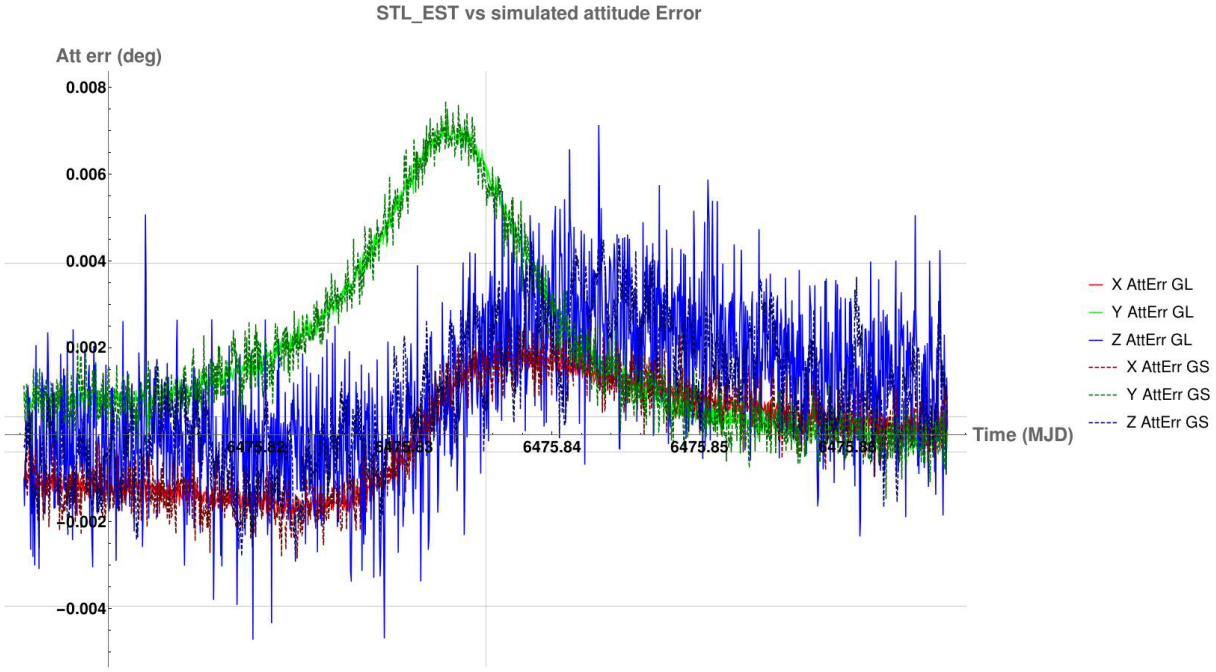

Figure 3: AME during nadir pointing with offset S/C axis (worst case gravity gradient), GS vs GL with gravity gradient model

3.3. Expected behavior in case of STR loss

One of the main issues of the GLE estimator is its limited robustness against STR outage periods, which can typically happen due to blindings, high S/C angular accelerations, poor STR field of view, etc. This is not a problem for the GSE which, in such a situation, can keep propagating the attitude based on the rate measurements from the gyros and can thus withstand long STR outage periods. The GLE, however, is left without any external measurement, and it is just a matter of time until the errors in the prediction model propagate up to an unacceptable attitude off pointing. Several mitigation measures were considered in the updated AOCS OBSW design and are discussed in Section 4.3. As a preliminary step, a worst-case estimation of how long the GLE could survive without measurements was performed. This analysis showed that an off-pointing of 0.5 °, corresponding to the High Gain Antenna half cone width, could be reached in as short as 15 s. One of the main contributions to this effect was the worst-case initial rate estimation error, happening during solar array repositionings.

3.4. Main conclusions from the feasibility analysis

The feasibility analysis yielded the following main conclusions:

- No reason existed to believe the performance of the GLE estimator of Rosetta, with identical implementation and tuning, would not be good enough for the MEX use case.
- Large APEs were to be expected during SA repositionings in GLE. This did not constitute a problem for science operations, during which the SA are kept at a fixed position.
- STR unavailability cases, even for short periods of time, had to be taken into account in the design process, since the attitude off-pointing with prediction-only model can increase very quickly.

Based on these conclusions, the adaptation of ROS gyroless estimator to MEX was considered feasible and the AOCS OBSW modification process was triggered.

4. SW modification design

4.1. Approach

The SW modification design process was driven by a short timeframe and a desire to minimize risk and therefore unrequired complexity to the maximum extent. In particular, a special effort was made to keep critical parts of the AOCS OBSW untouched (e.g., elements of the SW used in Safe Mode, FDIR, etc.).

The following general guidelines were adopted in the design of the AOCS OBSW modifications:

- Re-use of ROS elements to the maximum extent both for the AOCS OBSW as well as for the operational approach.
- The changes to the AOCS OBSW should be as simple as possible and only as complex as necessary. Additional ground constraints were preferred over additional complications of the OBSW.
- If the assessment of a certain design choice would require an unaffordable amount of time for analysis, then the point would be left open and a switch would be included in the OBSW to allow for later tuning of the system based on flight experience.

To minimise the risk that a STR loss of track could result in a worst-case absolute pointing error of 0.5° after a few seconds, thus causing loss of HGA communications, two autonomous mechanisms were implemented: a STR hot-swap mechanism, and a switch on of the gyros and transition to GSE in case of unavailability of either STR.

4.2. SW design and implementation

The AOCS OBSW of MEX (and ROS) is structured in different independent software objects. Each object is responsible for its own internal management and consistency, and thus handles its own state transitions through internal state automata.

Mainly two MEX AOCS objects had to be modified in order to incorporate the capabilities for the GL attitude estimation: the Stellar Estimator (STL_EST) and the Normal Mode Manager (NM_MGR).

The STL_EST encapsulates the attitude estimation functionality, i.e., it is in charge of collecting the measurements from the different sensors and running the Kalman filter processing, yielding an attitude and rate estimate. Its scheduling cyclically performs the prediction (8Hz) and update (2Hz) processes and makes the current estimates accessible to the mode. In the modified software, relevant parts of the ROS STL_EST were copied over to the MEX OBSW. Since this object is mainly in charge of the low-level computations, very little redesign was required.

The NM_MGR is a higher level SW object in charge of the full S/C control loop during nominal operations. It is organized in several submodes or phases with attitude guidance and controller tunings tailored to different use cases: one dedicated to Earth communication, one for science pointing and one for slews. The main part of the SW modification process was focused on this object. While in ROS the usage of the gyroless estimator was only possible through a specific phase of the NM_MGR, it was decided that, for MEX, the addition of a new independent automaton was more convenient. This would allow the NM_MGR to operate with the GSE or GLE regardless of the NM phase, thus decoupling the handling of the attitude estimator from the pointing mode selection. This approach also minimized the number of changes required in the ground operational concept. The new automaton inserted in the NM_MGR, called EST

automaton, is shown in Fig. 4. The EST automaton manages the transitions of the STL_EST object and related resources (gyros, STR units). It consists of the following four states:

- **GS (GyroStellar):** this is the automaton entry and default mode. It corresponds to a STL_EST operating in Gyrostellar mode. The S/C will never exit this mode unless Ground toggles a commandable switch. Leaving this switch off allows Ground to operate the S/C as before the SW update. When the switch is toggled, the automaton checks whether the STR is in tracking mode and the gyros have been available for a given number of consecutive cycles and, in such case, triggers an autonomous transition to GST.

- **GST (GyroStellar Transition):** this is a transition state in charge of initializing the gyroless estimator and ensuring estimator consistency before the final transition to gyroless. At transition to this state, the STL_EST starts running the gyroless estimator in parallel with the gyrostellar one. The automaton then performs a consistency check (checking for estimator state consistency, measurement availability, etc.) that needs to be successful for a number of consecutive cycles before allowing the final transition to gyroless. If the transition to GL is not triggered before a given timeout, the automaton falls back to GS. While in GST, the gyrostellar estimator is still the one used in the control loop.

- **GL (GyroLess):** in this state, the gyroless estimator is used by the AOCS control loop. Normally, following a transition to GL, the gyros are switched off. However, a Ground commandable flag allows keeping the gyrostellar estimator running in parallel. This feature was used for validation purposes in the first weeks of gyroless operations.

- **GLT (GyroLess Transition):** this state is entered autonomously when the gyroless estimator does not receive STR measurement updates for a given amount of time. It can also be triggered by ground command. At transition from GL, this state takes care of switching on the gyros and waits until they provide valid data. Once this is the case, the transition to GS is triggered, requesting the STL_EST to perform a transition to gyrostellar mode.

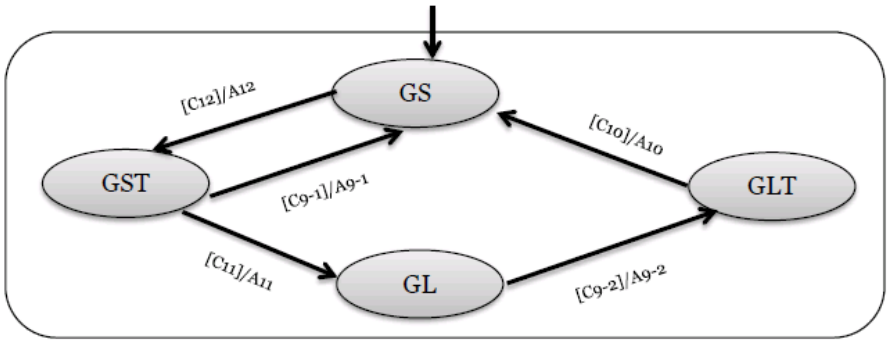

Figure 4: NM_MGR EST automaton

4.3. Protection against STR loss of tracking

As explained in the previous sections, one of the main issues with the gyroless attitude estimation is its quick degradation when the STR is unable to provide frequent measurements. To mitigate this risk, two additional capabilities were incorporated in the OBSW.

- **Autonomous STR swap:** MEX has two STR units which were operated in cold redundancy. This is however not enough for the gyroless estimator due to the long time

required to switch on and perform attitude acquisition with the redundant unit, so a hot redundancy mechanism, where both STRs are kept on and tracking, was put in place. When the EST automaton is in GL state and the STR in the control loop becomes unavailable, an autonomous swap to the redundant STR can be triggered if this mechanism is enabled by Ground. This process is fast enough to allow keeping the gyroless estimator in the control loop when one of the STRs loses track. The cost of this capability is the need to keep both STRs on at all times, however this could be afforded in terms of power budget.

- **Allow ground to command the maximum SA repositioning speed:** as shown by the preliminary performance analysis, the worst gyroless AME happens during SA repositionings. This error is one of the main contributors to the worst-case attitude error drift in case of STR unavailability, since it drives the worst case initial rate and attitude errors. As part of the MEX AOCS OBSW upgrade, the function to manipulate the maximum SA repositioning speed was made available to Ground as external TC. The expectation was that, by tuning this value, ground could adjust the magnitude of the AME spikes caused by the SA repositionings while still moving the arrays at a reasonable speed.

5. Gyroless estimator tuning

Because the GLE algorithm was replicated from Rosetta, the same approach was also followed for its tuning, as detailed in [4]. Following the Rosetta approach, two different techniques were used to get to a meaningful tuning of the covariance matrix:

- **Kalman tuning:** this approach is based on Kalman filter theory and uses the sensor and model error characterization to obtain a best estimate of the covariance matrix. This method depends on the performance characteristics of the STR and RWs, the physical properties of the S/C (mass properties) and the expected flight profile (attitude accelerations and rates).

- **Response time tuning:** this simpler approach uses a linearized mono-dimensional model of the estimator and tunes the corresponding second order filters based on response time considerations. In contrast to the first method, the only S/C characteristic that has an impact on this method is the STR performance.

In Rosetta, the results obtained from the first method were discarded because they yielded an unsatisfactory response time. For this reason, the final tuning values for ROS where obtained using the second method.

Three tunings were analysed for the MEX gyroless estimator:

- **Tuning A:** Kalman tuning based on noise error analysis
- **Tuning B:** response time tuning based on more recent STR performance data
- **Tuning C:** original ROS GLE tuning (response time tuning based on the original STR performance data)

Table 2 shows the obtained estimator response times around the different S/C axes for the different tunings. It can be seen that, as opposed to ROS, tuning A yields reasonable response times in the case of MEX.

Table 2: response times (63%) for the different tunings

Tuning A	
τ_{xy}	1.3 s
τ_z	4.1 s
Tunings B and C	
τ_{xy}	6.7 s
τ_z	6.7 s

The performance trade-offs are apparent in Fig. 5 and Fig. 6, which show the simulated AME for a Mars Nadir pointing profile with maximum gravity gradient. It can be seen that tuning A is more responsive, and thus damps the error due to the SA acceleration faster at the cost of having a higher frequency noise. Tunings B and C yield very similar results.

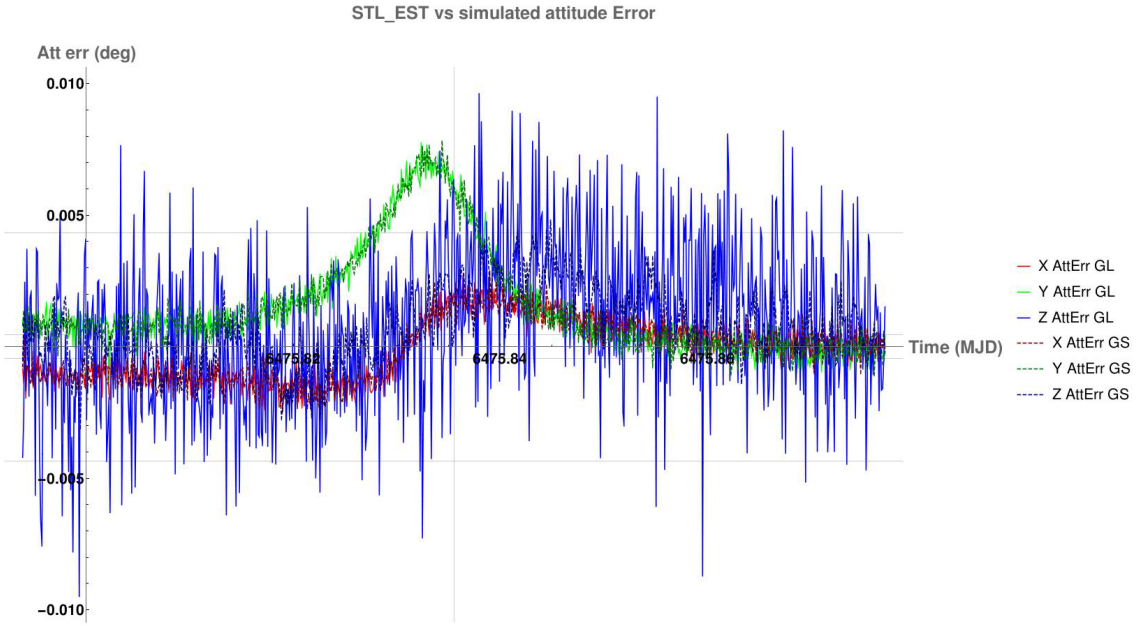

Figure 5: AME with Tuning A

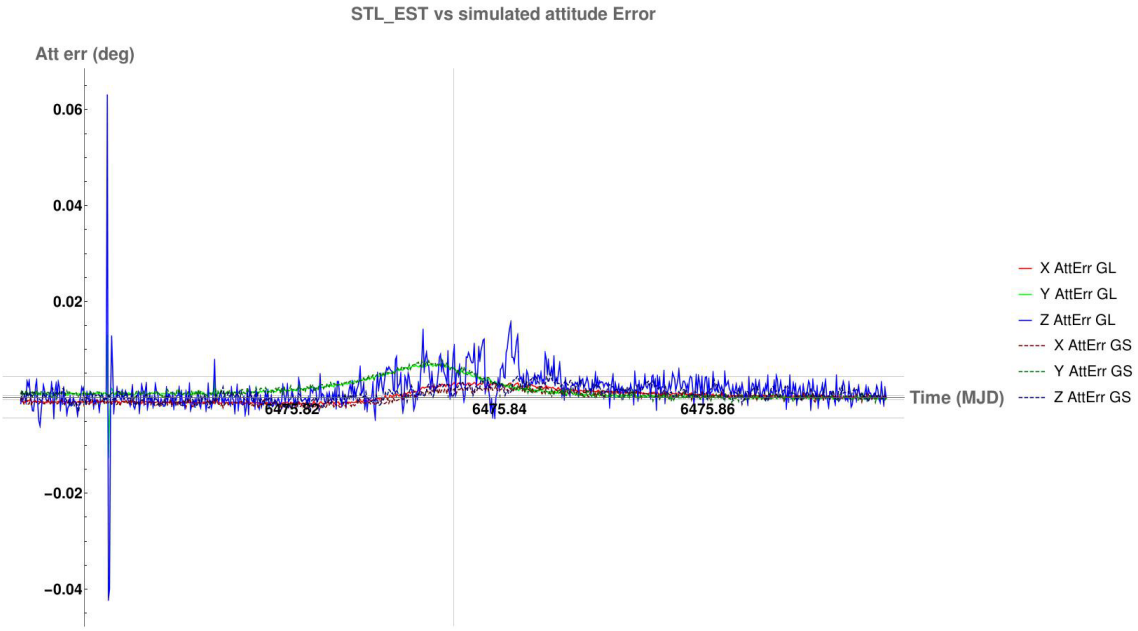

Figure 6: AME with tuning B (very similar to tuning C)

Based on this and other similar simulated performance comparisons, tuning C, i.e., the original ROS tuning was selected. The use of flight-validated parameters and the fact that the achieved simulated performance was good enough were considered the most important arguments in the selection. All the assumptions used in the ROS tuning were applicable to MEX, and thus, no strong reason to change it was identified. Although it was understood that a more responsive tuning like Tuning A could yield better results around SA repositionings, the pointing stability could have been affected. During science pointings, the SA are kept at a fixed position. Therefore, since the pointing performance around SA repositionings does not impact the science operations, it was decided to accept the behaviour of the original ROS tuning. Regarding tuning B, no relevant performance advantage was observed in the simulated data, which is why it was discarded.

6. Operational phase-in and in-flight results

The operational activities after the installation of the new OBSW proceeded in order of priority as follows:

- Check the S/C behavior during the S/C recovery after the OBSW reboot
- Check the S/C behavior in Normal Mode using GSE
- Check the new features of the software

For the third part, an incremental test plan, showed in Table 3, was defined. The following figures show some examples of the results obtained during the testing of the new features.

Table 3: GLE in-flight test plan

Test name	**Purpose**
Test 1	Switch on the gyroless estimator and check its outputs. The GLE is not in the control loop but run in parallel to the GSE
Test 2	Characterize the effect of the SA rotation at different maximum speeds on the GLE. The GLE is not in the loop but run in parallel to the GSE
Test 3	Put the GLE in the control loop for the first time. The S/C attitude guidance is kept Earth Pointing (i.e., quasi inertial attitude)
Test 4	Test the NM_MGR automaton transitions
Test 5	Perform a rotation around the HGA boresight in NM science phase with the GLE in the loop
Test 6	Perform a rotation around the HGA boresight in NM slew phase (different controller gains) with the GLE in the loop
Test 7	Characterize the effect of the SA rotation at different speeds on the GLE estimator with the GLE in the control loop
Test 8	Test the autonomous STR swap capability
Test 9	Test the GLE in the worst possible dynamical conditions (maximum attitude acceleration and rates, high gravity gradient torques)
Test 10	Put the GLE in the control loop while Earth pointing and switch the GSE off for the first time. Then trigger and test the transition back to GSE

Fig. 7 shows an example of the results obtained for Test 3. The gyrostellar estimator was kept running in parallel to the gyroless estimator, thus allowing for comparison and for a quick autonomous fallback in case of trouble with the gyroless estimator. It can be seen that the consistency between the estimators is very good. The gyroless control loop is stable and provides a similar performance in terms of APE.

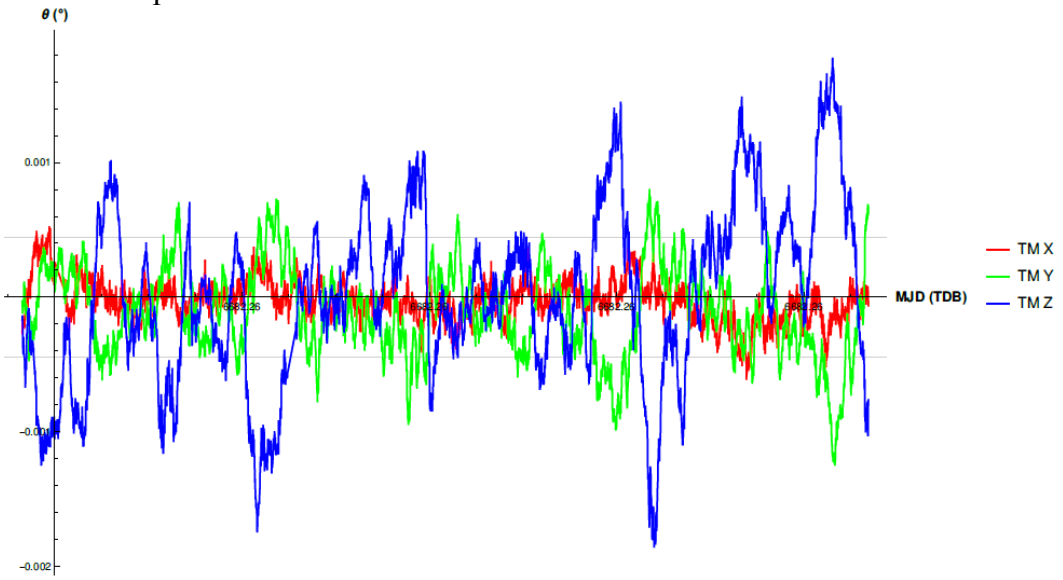

Figure 7: attitude error between GS and GL with GL in the loop in earth pointing attitude (STR frame)

As explained in section 3, the AME in GL is expected to be maximum during SA repositionings. Fig. 8 (corresponding to Test 7) shows the attitude error between GS and GL for a series of SA repositionings (marked with vertical grid lines) with two different SA speed settings, the initial one with a lower acceleration than the second one. The effect of increasing this acceleration is clearly visible in the AME.

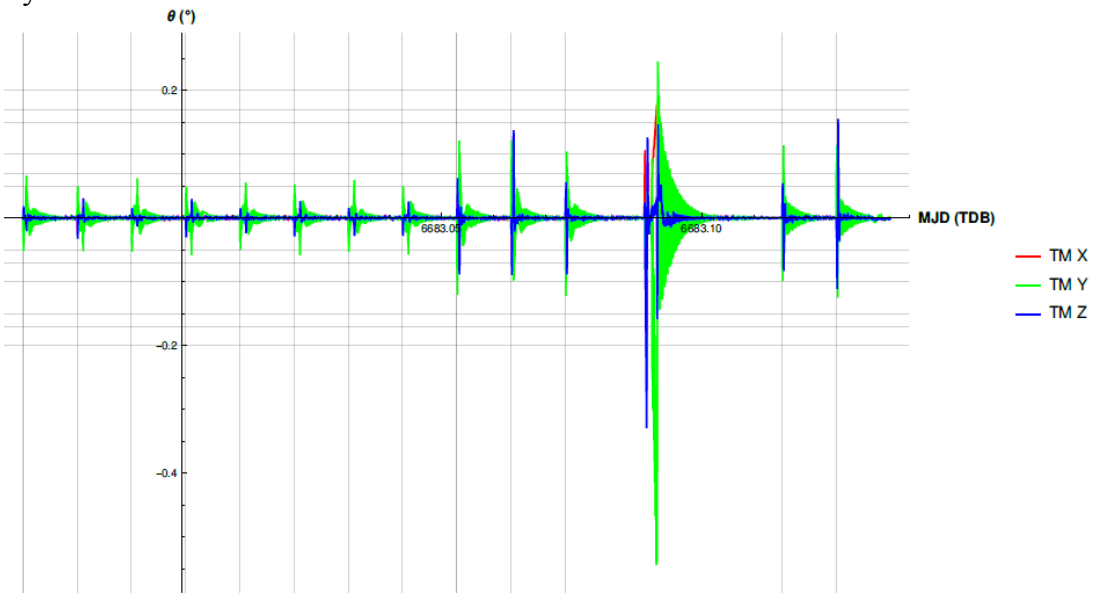

Figure 8: attitude error between GS and GL during SA repositionings with GL in the loop (S/C frame)

Fig. 9 shows the obtained attitude off pointing between the GS and GL estimated quaternions during a Nadir pointing pass during Test 9. The consistency between the estimators is again very similar to the results obtained in simulations.

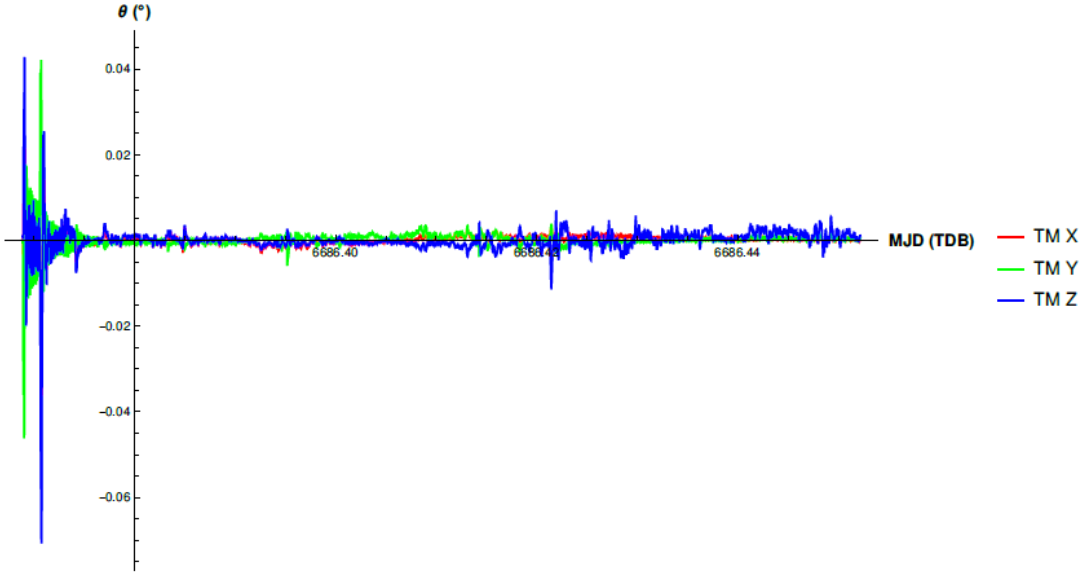

Figure 9: attitude error between GS and GL estimators during Nadir pointing (STR frame)

Conclusion

In 2017, it became evident that due to aging gyros the MEX mission would end by late 2018 unless a mean was found to reduce the gyro usage. At this time, the MEX AOCS did not allow such a reduction. However, because of the commonalities of the Rosetta and Mars Express AOCS, a feasibility analysis was performed in order to assess the possibility of incorporating the gyroless estimator available in the Rosetta AOCS into the MEX AOCS. Because the gyroless estimator on Rosetta was only meant to be used for quasi-inertial attitudes and low environmental torques, dynamical analyses had to be performed. The analysis showed the Rosetta GLE is adequate to support typical MEX science pointings (see section 3). Because of these results, a success oriented implementation plan was set in place by the MEX Flight Control Team (FCT). The present paper described the major tasks performed in Flight Dynamics, which were the software design and implementation (section 4) and tuning (see section 5). Other essential tasks, like software validation and uplink and activation of the software image, were performed by the FCT and are not covered in the present paper. It is also worth to mention that experts from Airbus, the SC manufacturer of MEX and ROS, reviewed the work, and provided valuable feedback and helped to make sure that topics were addressed in correct order of priority.

The updated MEX AOCS software was activated in April 2018. The observed pointing performance showed to be fully in line with the expected behavior from the dynamical simulations. Because of this, the ambitious schedule of rolling out and testing the new OBSW in a two-week window could be accomplished. After this period, MEX returned to routine operations with GLE in the loop. For the first few weeks, the GSE was kept running in the background to gain more confidence. Since then, MEX is operating with GLE in the loop. The GSE is only switched on for daily wheel offloadings (WOLs) and it will be the subject of future work to perform WOLs also with GLE in the loop.

The science return of the mission has not been materially degraded by the use of the GLE. The attitude of the spacecraft had to be constrained to avoid STR blindings, but since STR blindings

do not occur in the MEX Nadir pointing attitude, this is an acceptable restriction. In addition, occasional special pointings can still be supported with GSE.

In late 2018, Mars Express mission was extended for the years 2019 and 2020 and further extensions are envisaged. The work presented in this paper was instrumental in turning an expected end of mission into a multi-year extension.

References

1. C. Bielsa, J. M. García, M. Mueller, "Mars Express – Gyroless Operations – AOCS Software modifications and tuning", MEX-ESC-TN-5530, 1.1 (05/04/2018)

2. G.Mallier, C. Cazes, S. Ayache, E. Ecale, **"**Mars Express – AOCMS Software Requirements Document", MEX-MMT-RS-0387, 5.3 (25/09/2003)

3. C. Lacuisse, P. Regnier, "Rosetta Gyroless Stellar Estimation Function Definition and Justification", RO-MMT-TN-2009, 2.0 (26/02/2001)

4. C. Lacuisse, C. Juillard, P. Regnier, "Tuning of the Gyro-Stellar and Gyroless estimators", RO-MMT-TN-2090, 1.0 (05/07/2000)

5. P.Regnier, J. Touaty, "Re-tuning of the Gyro-stellar estimator", RO-MMT-TN-2223, 1.0 (06/12/2004